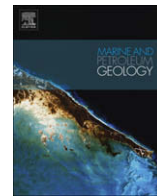




Contents lists available at ScienceDirect

Marine and Petroleum Geology

journal homepage: www.elsevier.com/locate/marpetgeo

Distinct activity phases during the recent geologic history of a Gulf of Mexico mud volcano

I.R. MacDonald^{a,*}, M.B. Peccini^b^a Department Physical and Environmental Sciences, Texas A&M University – Corpus Christi, 6300 Ocean Dr., HR121, Corpus Christi, TX 78412, USA^b I.M. Systems Group/NOAA Fisheries, 1315 East-West Highway, Silver Spring, MD 20910, USA

ARTICLE INFO

Article history:

Received 2 June 2008

Received in revised form

1 December 2008

Accepted 14 December 2008

Available online xxx

Keywords:

Mud volcano

Brine pool

Seep mussel

Radiocarbon age

Eruption

Bathymodiolus childressi

Laser line scan

Sub-bottom profile

ABSTRACT

Laser line scan imaging and chirp sub-bottom profiling were used to detail the morphology of a submarine mud volcano and brine-filled crater at 652 m water depth in the northern Gulf of Mexico. The mud volcano has a relief of 6 m and a basal diameter of about 80 m. The feature comprises a central, brine-filled crater (253 m²) surrounded by a continuous bed of methanotrophic mussels (*Bathymodiolus childressi*) covering 434 m² and a patchy bed covering an additional 214 m² of the periphery. The brine pool was mostly <2 m deep, but there were two holes of >28 m and 12 m deep, respectively at the northern end of the pool which emitted continual streams of small clear bubbles. Sub-bottom profiles indicated three distinct strata beneath the present surface of the mud volcano. Integration of 17 profiles shows that the mud volcano has been built in at least three successive stages: the lowest stage deposited 35,400 m³, while the middle and upper stages deposited 7700 and 20,400 m³, respectively. Piston cores were taken at the northern edge of the mussel bed and a site ~100 m southwest of the pool. Mussel and lucinid shells were recovered from the closer core, lucinid shells from the distant core. A mussel shell from 3.4 m sub-bottom had a $\Delta^{14}\text{C}$ age of 16.2 ka. Mixture of modern carbon with “carbon dead” reservoir material would produce actual ages ~2 ka less than the radiocarbon ages.

© 2008 Elsevier Ltd. All rights reserved.

1. Introduction

Submarine mud volcanoes are a common feature of the northern Gulf of Mexico continental slope (Milkov, 2000), where sediment loading (Bouma and Roberts, 1990), salt diapirism (Reilly et al., 1996), and over-pressured hydrocarbon reservoirs (Neurauter and Roberts, 1994) promote seabed fluid flow and diverse expressions of lumps, mounds, craters, and mud breccia. Eruptive discharge of massive volumes of material has been deduced from seismic evidence showing large craters and steeply sided cones (Prior et al., 1989). The process has also been observed directly as broad mud flows with attendant gas and fluid escape (Roberts and Neurauter, 1990).

Evidence for repeated episodic eruptions of mud volcanoes in Gulf of Mexico and elsewhere comes largely from inferences made during periods of quiescence or reduced discharge where different “generations” can be compared from seismic and observational evidence (Neurauter and Roberts, 1994), or “terrains” associated separate flow events can be mapped (Dimitrov, 2002; Milkov et al.,

1999; Sager et al., 2003). Potential transport of greenhouse gas (methane) from mud volcanoes to the atmosphere has been reviewed by a number of authors (Dimitrov, 2002; Kopf, 2002, 2003; Kvenvolden and Rogers, 2005). Eruptions of a Gulf of Mexico mud volcano were associated with repeated fluid temperature excursions (to 47 °C) and greatly expanded oil flow to the sea surface (MacDonald et al., 2000). These results indicate that under conditions of eruption, the flux of greenhouse gases to the atmosphere can be enhanced, either through large volumes of gas burst through the water column (Judd et al., 2002, and references therein), enhanced transport of gas and oil (Leifer and MacDonald, 2003), or a combination of both processes. However, data on the frequency, timing, and variability of eruption for submarine mud volcanoes is limited. Even with close observation, it is difficult to quantify changes in discharge rates of mud and gas at submarine mud volcanoes despite indications of highly variable discharges in the geologic past (Feseker et al., 2008; Milkov et al., 1999; Shilov et al., 1999). Better evidence for the seismic or stratigraphic characters associated with eruptions will contribute to the recognition of eruption events.

The ecological importance of submarine mud volcanoes has been widely noted. Mud volcano fluids are a nutrient source for microbial communities (Joye et al., 2005; Sass et al., 2001; Yakimov

* Corresponding author. Tel.: +1 361 825 2234; fax: +1 361 825 2025.

E-mail addresses: ian.macdonald@tamucc.edu (I.R. MacDonald), mike.peccini@noaa.gov (M.B. Peccini).

et al., 2002), while chemosynthetic host metazoans and associated heterotrophic species colonize the substrata created by repeated mud flows (Gebruk et al., 2003; Huguen et al., 2005; MacAvoy et al., 2002; Olu-Le Roy et al., 2004; Smith et al., 2000). Because the chemosynthetic metazoans require tens of years to reach maturity (Nix et al., 1995; Smith et al., 2000), successful colonization of mud volcanoes is challenged if frequent eruptions bury or dislodge colonists (Roberts and Carney, 1997). The persistence of a dense chemosynthetic community at a mud volcano indicates recent dormancy for the colonized portion of the feature.

Where active mud or fluid discharge is not evident, the physical characteristics of mud volcano fluids can be an indicator of a feature's relative activity. Joye et al. (2005) suggest that dormant mud volcanoes develop thermoclines as heat is lost from the upper layers of the pool. Hypersaline fluids have frequently been reported from submarine mud volcanoes, including numerous examples from the Gulf of Mexico (MacDonald et al., 1990; Roberts and Carney, 1997) and the Mediterranean Sea (Aloisi et al., 2000; Charlou et al., 2003; Dimitrov and Woodside, 2003; Fitzsimons et al., 1997; Woodside and Volgin, 1996; Yakimov et al., 2002), where hypersaline fluids range from a mud-brine slurry to sediment-free brine (Huguen et al., 2005). However, not all brine-filled seafloor pools are generated by mud volcanism. Dissolution of shallow salt can create channels of flowing brine (Aharon et al., 1992) that can fill large depressions. The most substantial brine pool in the Gulf of Mexico is Orca Basin, which is some 25 km wide and 200 m deep (Shokes et al., 1977); it was created by infilling from surrounding salt diapirs rather than volcanic discharges (Brooks et al., 1990). Seafloor brines are potentially lethal for mobile fauna (Kvitek et al., 1998; MacDonald, 1992) and hypersaline, anoxic conditions may promote preservation of fossil remains with characteristic taphonomy (Parsons-Hubbard et al., 2008).

This paper will present¹ detailed and fine-scale data from an optical and seismic survey of a small mud volcano known as Brine Pool NR-1 (MacDonald et al., 1990). The feature has not erupted since its discovery in 1989 and, from the evidence of its chemosynthetic community, has probably been dormant for 100s of years prior to that. However, the evidence shows the morphology of the feature as been altered by events over the past ~ 15 ka.

2. Materials and methods

2.1. Site survey methods and sampling

Brine Pool NR-1 is located in water depths of 650 m in block 233 of the Green Canyon lease area approximately 250 km southwest of the Mississippi River Delta. The site was surveyed with a U.S. Navy nuclear submarine, NR-1, which has been regularly made available for scientific use (Babb et al., 1993; Parsons et al., 2005). For these surveys, submarine NR-1 was equipped with an SM-2000 laser line scan system and an Edgetech X-Star 12–28 kHz chirped sub-bottom profiler. The laser line-scanner is an imaging system that processes backscatter from a green laser projected onto the seafloor by a rotating prism to assemble a high-resolution optical image (MacDonald et al., 1997).

Navigation of the NR-1 was conducted with an inertial navigation system that was routinely corrected with fixes from a support

ship. For the laser line scan survey, NR-1 was piloted on a series of east–west tracklines while maintaining an altitude of 5 m above the bottom. These tracks were focused in a 40 × 40 m box centered on the pool (Fig. 1A). For the sub-bottom survey, the pool and its surroundings were transected by a series of ~125 m tracklines crossing north–south, east–west, northwest–southeast and north–east–southwest. During the sub-bottom transects, NR-1 was piloted at a constant water depth of 630 m to preserve the profile of the bottom (Fig. 2).

Additional materials (shell samples) were collected with the submersible Johnson Sea-Link and by piston coring from the R/V GYRE. Cores were maintained in butyrate liners in cold storage until the liners were split for interpretation. Navigation of the piston cores was accomplished by rigging the corer to release a small anchored float on impact with the bottom. Submersible Sea-Link subsequently relocated the floats and determined their position with respect to the brine pool by means of ultra-short baseline acoustic navigation.

Submarine Johnson Sea-Link was used to conduct a lead-line survey of the brine pool, which due to its acoustic contrast and poorly defined bottom resists acoustic depth determination. A small winch mounted on the front of the submersible in view of the operators was used to lower a weight into the brine pool. Depth was determined by counting marks on the line until it was seen to go slack. Depths were taken at regular intervals along imaginary lines between marks on the edges of the brine pool. A total of 28 depths were taken. The maximum depth, which only recorded at two points, probably exceeded 30 m length of the lead line.

2.2. Data processing and analysis

Laser line scan images were recorded on analog videotape, which showed the real-time display of the bottom as NR-1 transited the feature. For assembly as a mosaic, frames of video were digitized and assembled into seamless image strips 1024 pixels wide. Individual strips were length adjusted to conform to the NR-1 navigation records using ER-Mapper[®] image processing software. The strips were filtered to remove cosine effects of the rotating laser and to remove noise. Strips were mosaicked into a single image using warping routines of ER-Mapper to ensure feature matches at seams.

X-Star sub-bottom profiles were recorded as digital image files. The vertical scale was determined from the default sound speed setting for marine sediments and assumed a common depth point of 630 m based on the submarine's assigned water depth. The horizontal scale was adjusted so that time-marks on the profile aligned with the submarine's navigation records. Crossing points for the edge of the pool provided benchmarks for aligning the tracklines. The bathymetric contours were calculated by integrating the bottom depths and NR-1 navigation records. Sub-bottom strata were manually digitized in the X-Star profiles and then surface-fit using PV-Wave[®]. Strata that appeared in a minority of the tracks were excluded from analysis. Integrated volumes of each successive stratum were compared for volume calculations.

Piston cores were interpreted and shell fragments were recovered for identification and radiocarbon dating. Burial depths were recorded relative to the uppermost level of the cores. The shell fragments were carefully abraded to remove cements prior to analysis. Radiocarbon and stable carbon isotope ratios were measured at the National Ocean Sciences Accelerator Mass Spectrometry Facility². Radiocarbon results are reported as percent

¹ Preliminary versions of these results were previously distributed as portions of a technical report MacDonald, I. R., R. Arvidson, R.S. Carney, C.F. Fisher, N.L. Guinasso Jr., S. Joye, P. Montagna, J.W. Morse, D.C. Nelson, E. Powell, W. Sager, R. Sassen, S. Schaeffer and G.A. Wolff, Eds., 2002. Stability and Change in Gulf of Mexico Chemosynthetic Communities: Final Report. New Orleans, LA, U.S. Dept. Interior, Minerals Management Service, Gulf of Mexico OCS Region, Contract 14-35-001-31813.

² Details regarding the repeatability and precision of results obtained by the National Ocean Sciences Accelerator Mass Spectrometry Facility (NOSAMS) can be found at <http://www.nosams.whoi.edu/>.

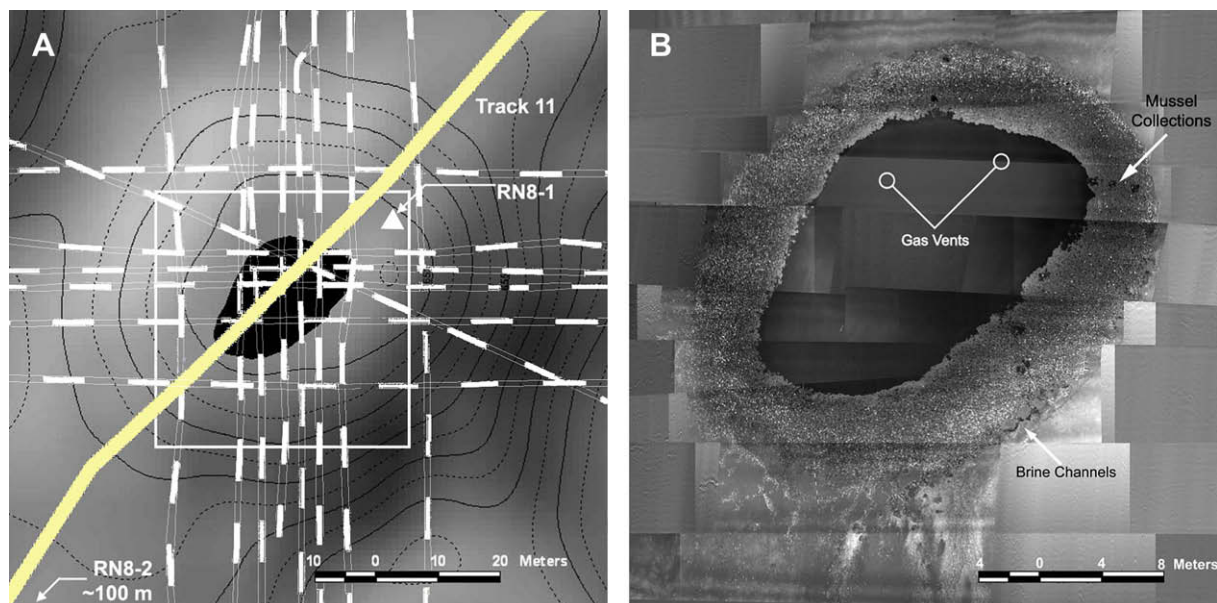


Fig. 1. Surface view of Brine Pool NR-1. A. Bathymetry of mud volcano and central brine pool (topmost is north). Tracklines show sampling plan for sub-bottom survey showing lines focused on pool and locations of piston core samples. White outline shows boundary of mosaic. B. Laser line scan mosaic of pool and mussel bed. White circles are active gas vents. Arrow shows brine channels in stable location and some of the divots generated by collection of mussels.

modern carbon and calculated ^{14}C age. Stable carbon isotope values are reported as $\delta^{13}\text{C}_{\text{‰}}$ compared to Pee Dee Belemnite standard.

3. Results

3.1. Surface features

The laser line scan mosaic shows that Brine Pool NR-1 is a precisely defined pool surrounded a well-developed chemosynthetic community that is dominated by a large biomass of methanotrophic mussels (*Bathymodiolus childressi*). Several regions were readily distinguished in the full resolution image (Table 1). Open brine was clear and relatively free of suspended mud. Previous results (MacDonald et al., 1990), replicated during this survey, show that the brine has a salinity of 121 PSU and is about 2 °C warmer than ambient seawater (which is ~7 °C) in the upper layer. At depths greater than 5 m below the brine–seawater interface, the temperature increases to over 17 °C (Joye et al., 2005). The edges of

the pool are defined by tightly clustered mussels (Fig. 1B), but brine extends as a thin layer underlying the inner part of the mussel bed. Mussels appear to thrive where they are able to keep their siphons above the brine, but may slide under the brine and succumb on the inner most edge. Dead mussels, as well as fish and other species, lie under the brine on the bottom of the pool, where they are commonly observed from submersibles and can be faintly seen in the laser line scan mosaic. The radial extent of brine within the encircling mussel bed defines an inner portion of the bed that includes large, healthy individuals as well as numerous juveniles (Nix et al., 1995; Smith et al., 2000). Outward from the brine, the mussels are older, less tightly clustered, and include a higher fraction of dead shells. Collections of mussel specimens during the years previous to the survey created circular divots in the mussel bed that did not readily fill in with new colonists (Fig. 1B arrows).

The mud volcano has a sub-circular cone with a relief of 6 m and a basal diameter of about 80 m. The crest of the cone is defined by an elliptical contour at 652 m, which has an east–west elongation of

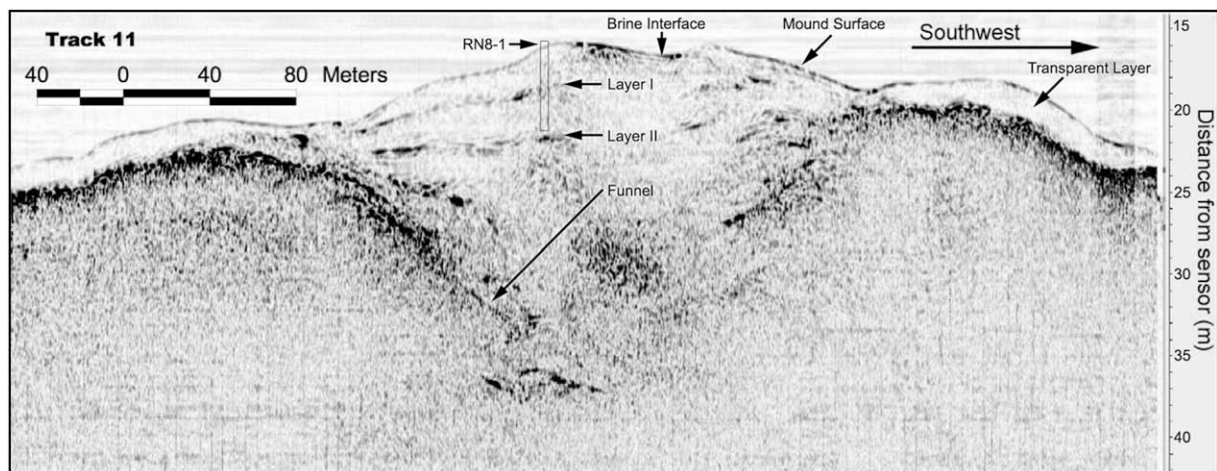


Fig. 2. Sub-bottom of pool and mud volcano. Example shows Track 11 of X-Star 12–28 kHz chirp profile through center of pool. Labels show present-day surface, interpreted layers, and approximate penetration of piston core RN8-1.

Table 1

Areas of brine pool and associated mussel bed calculated from laser line-scan mosaic.

Site Characteristic	Area (m ²)
Contiguous mussel bed	434
Peripheral mussel beds	214
Open brine	253
Total area of mosaic	1658

about 4:3. The pool abuts the southern edge of this contour (Fig. 1A) and there is an elevated berm enclosing the north end of the mussel bed. Therefore, the brine seeps out through the southern edge of the mud volcano, where the mussel bed is extended as linear striations of shells, white precipitates (probably amorphous sulfur), and bacterial mats. Scalloped brine channels along the southeastern edge of the mussel bed correspond to features observed 10 years earlier. The eastern and southeastern slopes dip well below the base of the cone. The greater area within ~250 m from the pool includes other small pools, pockmarks, and aggregations of mussels and chemosynthetic tubeworms (*Lamellibrachia luymesii*).

3.2. Subsurface features

The X-Star profiles across the flanks of the cone show a high-contrast interface underlain by an acoustically transparent layer 2–3 m thick (Fig. 2). There are irregular lobes on the north and the southern beyond the edges of the cone where the transparent layer is thicker. The lobes appear to be debris ejected from the diatreme during periods of activity. This impression is reinforced by a strongly reflecting layer that converges as a funnel-like form beneath the crest of the cone. Within the cone, there are at least two distinct and laterally contiguous layers that converge at the edges of the funnel. There are no distinct strata below the funnel layer. The brine and possibly the mussel bed appear as a darkly contrasting surface reflector; however the sub-bottom below the brine has chaotic appearance without clear strata or features. The strata evident in track 11 (Fig. 2) were reasonably continuous among the other 16 tracklines that transected the pool, cone, and surrounding benthos (Fig. 1A).

The lead-line survey of the pool found a brine depth of 0.5–1 m over the southern end of the open brine. The brine was initially

translucent, with bottom features discernable until the survey roiled the bottom. Much greater depths were encountered at three positions along the northern edge of the pool. At two adjacent points, the entire 30 m line was played out from the winch without finding bottom. A third point encountered a saddle of 4 m depth and a fourth point found a depth of 12 m (Fig. 3A). Two continuous streams of clear bubbles were observed escaping from the deep holes. These bubble streams had been noted on all previous visits to the pool.

By tracing the sub-bottom layers in the individual X-Star profiles (e.g. Fig. 2), and interpolating between profiles, it was possible to approximate two of the sub-bottom strata between the surface and the base of the funnel (Layers I and II in Fig. 3B). The depth from the present-day surface of the pool to the focus of the funnel is approximately 18 m. So ratio of the depth of the funnel to the relief of the cone above the seafloor is about 3:1. A third sub-bottom layer was evident in a few of the profiles (e.g. track 11), but was absent in others. It was therefore not calculated. From comparison of the surfaces, we calculate that there is 35,400 m³ of sediment between the funnel and layer II, 20,400 m³ between layer II and I, and 7700 m³ between layer I and the present surface. The total volume of the funnel and cone is 63,500 m³.

3.3. Piston cores and radiocarbon dates

Core RN8-1 was collected approximately 5 m north of the mussel bed and recovered a 5.2 m core. Because the strata dip steeply on the edge of the pool, it was difficult precisely to match layers in the cores to layers in the X-Star profiles. However there were two relatively indurated layers in core RN8-1. These layers were ~1 m and ~3.5 m sub-bottom (Fig. 4). Two small mussel shell fragments were recovered in the upper section of RN8-1 and a third mussel shell was recovered from 3.4 m sub-bottom. A large lucinid clamshell and a smaller fragment, probably from a vesicomid clam were recovered at 0.7 and 3.7 m, respectively.

Core RN8-2 was collected about 100 m southwest of the pool and recovered a 4.2 m core. Its position is approximate because the navigation fix on the float released by the core was uncertain. Poorly consolidated sediments at the core top included several mudstones. Two small shell fragments from lucinid clams were

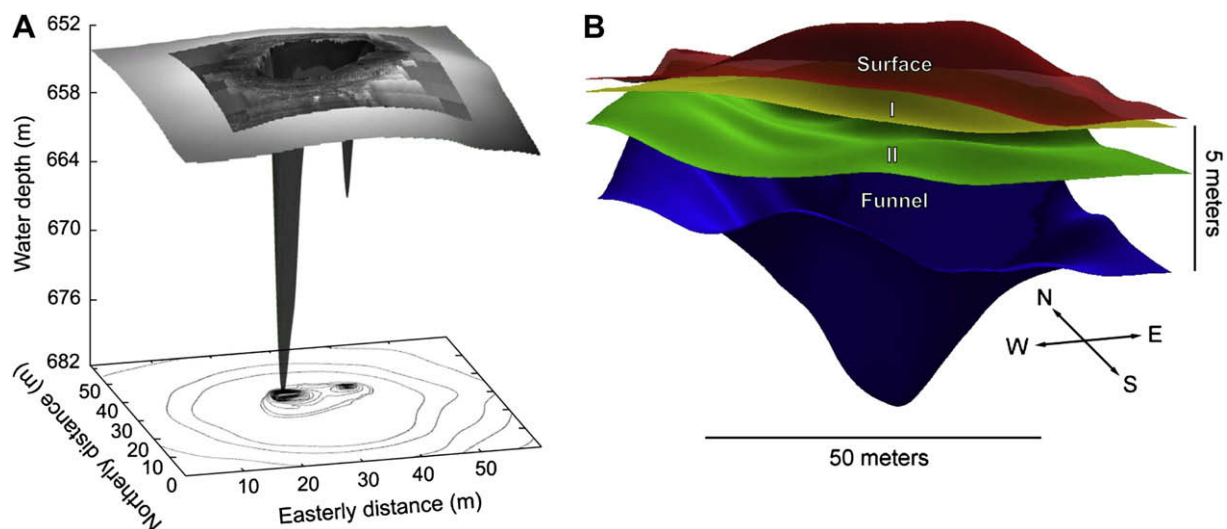


Fig. 3. Renderings of surface and sub-bottom features. A. Laser line scan mosaic draped over pool depth illustrates the relative scale of the surface expression and the deeply penetrating shafts. B. Rendering of sub-bottom layers shows complex mud flow patterns for previous mud volcano surfaces.

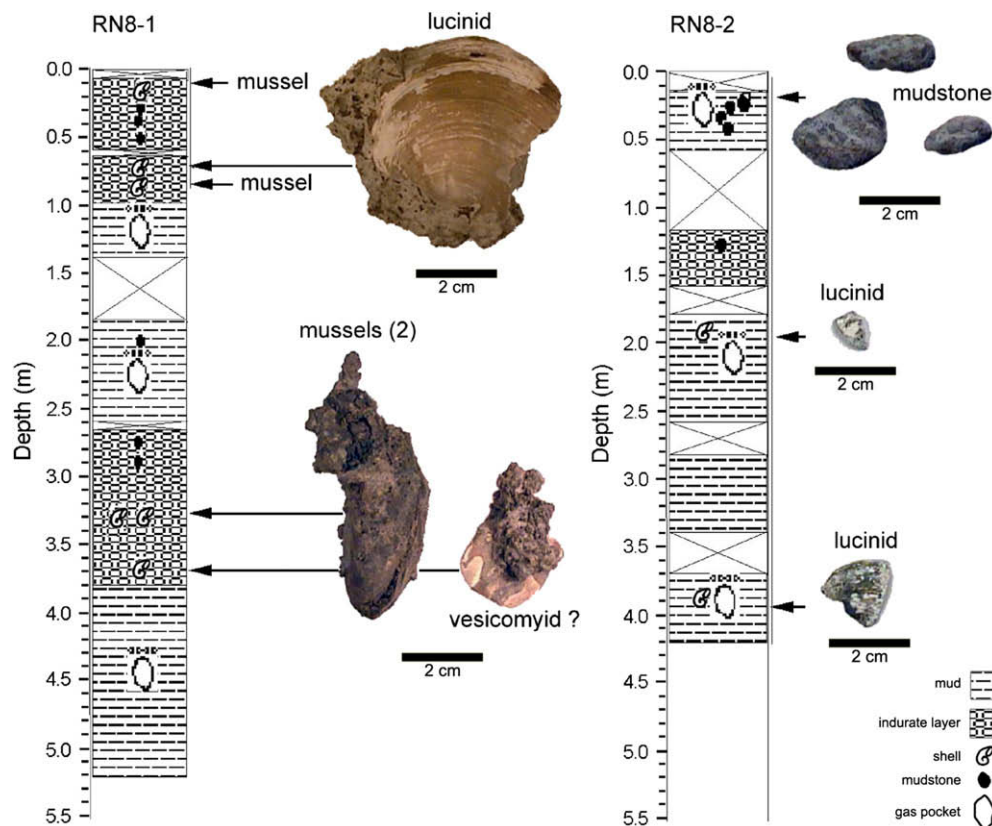


Fig. 4. Descriptions of piston cores collected at GC233 study site (see Fig. 2 for locations). The larger shells or shell fragments are depicted with their positions within the cores indicated. See Table 2 for ^{14}C ages of shells. Sediments comprised stiff clay or looser mud with gas pockets.

recovered at 1.8 and 4.0 m sub-bottom, respectively. The gas expansion voids in RN8-2 made it difficult to determine sub-bottom depths for the core.

Radiocarbon ages of the shell fragments (Table 2) were, with one exception, progressively greater with increasing depth. Mussel shells, diagnostic of a community sustained by methane bubbles or methane-rich brine were found near the pool (RN8-1), but not at the core taken away from the pool. The maximum radiocarbon age of the mussels was 16 ka, however this age must be compared with radiocarbon ages of 2 ka for living mussels taken from the pool edge and from another hydrocarbon seep mussel bed about 20 km away

(Bush Hill). Interestingly the living mussel shells were aged at the umbo (oldest part of the shell) and at the growth margin (youngest part of the shell). The difference in radiocarbon age for both these specimens was 200 y between the earliest and latest deposition of shell material.

A lucinid clamshell was recovered from 0.7 m in RN8-1. This specimen was anomalous with respect to its radiocarbon age (17.4 ka), which is substantially older than specimens from adjacent strata, and its stable carbon isotope ratio ($\delta^{13}\text{C} = -22.89\text{‰}$), which is an order of magnitude more negative than any other specimen in the collection.

Table 2

Carbon dates (accelerator mass spectrometer) for shells from the brine pool (GC233) and a nearby reference site (GC185). Samples collected by the Johnson Sea-Link submersible were two living specimens with respective lengths of 120 mm (GC233 – collected from present-day mussel bed at Brine Pool NR-1) and 90 mm (GC185 – collected from Bush Hill at 540 m depth, N27°47', W91°30') that were subsampled at the umbo and at the margin to distinguish minimum and maximum ages. Stratum depth indicates depth of specimen from sediment surface.

Site (Station)	Collection Method	Stratum depth (m) (specimen type)	Modern C	^{14}C Age (yBP)	Error (y)	$\delta^{13}\text{C}_{\text{‰}}$
GC233	Submersible	0.0 (mussel umbo)	77.78%	2020	35	-6.77
GC233	Submersible	0.0 (mussel margin)	75.86%	2220	35	-7.77
GC185	Submersible	0.0 (mussel umbo)	80.27%	1760	40	-1.66
GC185	Submersible	0.0 (mussel margin)	78.44%	1950	35	-2.46
GC233 (RN8-2)	Piston core	1.80 (lucinid)	18.11%	13750	35	-2.78
GC233 (RN8-2) ^a	Piston core	1.80 (lucinid)	18.00%	13750	30	-2.65
GC233 (RN8-2)	Piston core	4.00 (lucinid)	15.79%	14850	35	-1.55
GC233 (RN8-1)	Piston core	0.05 (mussel)	40.45%	7270	40	-1.97
GC233 (RN8-1)	Piston core	0.70 (lucinid?)	21.84%	17450	55	-22.89
GC233 (RN8-1)	Piston core	0.85 (mussel)	11.41%	12200	35	-1.11
GC233 (RN8-1)	Piston core	3.40 (mussel)	12.34%	15800	40	-2.3
GC233 (RN8-1)	Piston core	3.40 (mussel)	13.95%	16200	50	-5.16
GC233 (RN8-1)	Piston core	3.69 (vesicomyid?)	13.29%	16800	45	6.07

^a Replicated analysis.

4. Discussion

The elevation of the mud volcano, sediment slides, and bacterial mats on the downslope (southern) end of the pool, and a raised dike around the upslope (northern) edge of the pool are among the abundant visual evidence that the pool was excavated by vigorous eruption. The persistence of a mussel community, developed in the present day to a continuous band that completely surrounds the pool on the level margins of the crater, is strong evidence for conditions that have favored chemosynthetic animals over an extended time (Table 1). The highly ordered distribution of mussels, which features a sequence of life history stages from the mixture of recruiting juveniles and adults on the inner edge to the segregated adult assembly on the outer edge (MacDonald et al., 1990; Nix et al., 1995; Smith et al., 2000), is an elegant example of the capacity for concentration gradients to shape chemosynthetic communities. Similar gradients may be preserved in the fossil records of ancient seeps (Parsons-Hubbard et al., 2008; Peckmann and Thiel, 2004).

Eruption of the brine pool, even if it was confined to a single outflow channel, would drastically perturb the spatial integrity of the mussel bed and associated features (e.g. small brine channels Fig. 1B). Comparison of the present laser line scan mosaic with previous mapping shows that brine channels and distinctive mussel clusters remain as stable features for years. Large adults reach may reach maximum size at ages of ~200 y. Additionally, the slow recovery of gaps in the mussel bed created by sample removal up to 10 y prior to the line-scan survey indicates that the spatial features of the mussel bed are the result of long development. These lines of reasoning suggest that the mud volcano has been dormant during recent geologic time.

From the bathymetric and sub-bottom records, it is evident that the pool and surroundings have a complex three-dimensional structure. Brine Pool NR-1 is a mud volcano, as defined by Huguen et al. (2005) in that it is a lens-shaped body built up by successive flows. However, it is a relatively small and homogeneous feature compared to mud volcano complexes from the Barbados accretionary prism (Lance et al., 1998), the Nigeria margin (Graue, 2000), Hakon Mosby mud volcano (Milkov et al., 1999), and examples from the eastern Mediterranean (Charlou et al., 2003; Olu-Le Roy et al., 2004). In this context, the sequence of Brine Pool NR-1's activity is perhaps easier to delineate that it would be if there were multiple vents and overprinted mud flows.

Our data show that the mud volcano formed by repeated eruptions of fluidized mud from a single, focused piercement of the seafloor. It is unclear whether the entire volume of the funnel was excavated with a single eruption or by repeated events. The width of the spans the base of the mud volcano, exclusive of the debris lobes and maximum depth funnel is about 15 m below the surrounding seafloor. Ejected material would not form a stable surface within the sloping pit until the mud volcano was built above the level of the surrounding seafloor. This is evident from the convergence the present-day surface with layers I and II at the edge of the funnel (Figs. 2B and 3B). It seems probable that deeper layers were formed prior to layers I and II, but not until the formation of a stable, level surface, would a mussel community have been established. We further speculate that older mud flows may have exited the pool to the north until the accumulation of material created a dike that began forcing the flows to exit in a southerly direction. Examining Fig. 2, it seems possible that additional eruptions might construct a dike on the southern side of the funnel and reverse the flow direction. Fig. 3B suggests that each layer would have a distinctive pattern and direction of mud flows.

The pool maximum depth approximates the maximum depth of the funnel (Figs. 2 and 3A, B), this shaft is much narrower than surface pool, probably less than 10% of the pool width. Existence of

a second shaft suggests that the vent was originally bifurcated and possibly became blocked by debris. Continued venting of gas suggests that there is still some charge in the sub-bottom plumbing; it is clearly dormant rather than extinct.

Radiocarbon dating for seep fauna is problematic due to contamination of "dead" carbon from reservoir sources as well as seawater carbon (Aharon et al., 1997). Values of $\delta^{13}\text{C}$ from -7.77 to 1.11‰ for specimens that are depleted in ^{14}C relative to modern seawater due to carbon sourced from the ^{14}C -free hydrocarbons. The radiocarbon ages of living specimens analyzed (1.8–2.2 ka) is consistent with a mixed carbon source and consistent with previous radiocarbon dating of living mussels (Aharon et al., 1997). The ^{14}C ages for mussels recovered from the cores are probably 2 ka greater than actual ages. This is not the case for the lucinid found in the upper section of core RN8-1 (Fig. 4, Table 2). In this specimen, the ^{14}C age (17.4 ka) is greater than any of the other specimens (including other lucinid shell fragments) and its $\delta^{13}\text{C}$ value of -22.89 indicates a chemosynthetic carbon source. Although the Lucinidae are a highly diverse family (Taylor and Glover, 2006), there is scant evidence for methanotrophic symbionts. This specimen may have been transported to the site or exhumed from deeper levels.

Seep mussels (*B. childressi*) require methane and a stable substratum on which to grow. Frequent eruptions or mud flows would prevent the establishment a mussel population. Existence of a mussel population indicates a period of relative dormancy. Radiocarbon dating of mussels and other bivalves to 16 ka at a stratum below the present mussel bed suggests that there was a period relative dormancy in late Pleistocene (Table 2, Fig. 4). Recovery of a mussel shell with 7 ka radiocarbon age from the upper 5 cm of core RN8-1 indicates that presence of stable strata capable of supporting mussel colonization dating from early Holocene. The present dormant stage may have prevailed for several thousand years. This is relatively recent compared to 750 ka ages described for mud volcanoes of the western Atlantic (Lance et al., 1998).

In conclusion, Brine Pool NR-1 is a small mud volcano formed in late Pleistocene that has been largely dormant for a substantial portion of the Holocene. The early sequence of eruptions produced chaotic structures as extruded material settled into the crater. As the crater filled, the vent became increasingly narrow. When the discharged material reached the level of the surrounding seafloor, construction of a lens-shaped body could proceed with a series of mud flows. These flows produced indurate layers visible in sub-bottom profiles. Evidence from piston coring and radiocarbon dating shows that these layers have been colonized by methanotrophic mussels for at least 14 ka. If new, even minor, eruptions of this mud volcano were to occur in future, disruption of the existing mussel bed would offer clear evidence for the extent and timing of discharge.

Acknowledgements

This work was supported by contracts from the Minerals Management Service, New Orleans office (Contracts 14-35-001-30555 & 14-35-001-31813) and the NOAA National Undersea Research Program, University of North Carolina Center. We gratefully acknowledge the assistance of Chang Shik Lee for interpretation of piston core samples. We thank the crews of the submarines NR-1 and Johnson SEA LINK for outstanding assistance and support.

References

- Aharon, P., Graber, E.R., Roberts, H.H., 1992. Dissolved carbon and $\delta^{13}\text{C}$ anomalies in the water column caused by hydrocarbon seeps on the northwestern Gulf of Mexico Slope. *Geo-Marine Letters* 12, 33–40.
- Aharon, P., Schwarcz, H.P., Roberts, H.H., 1997. Radiometric dating of submarine hydrocarbon seeps in the Gulf of Mexico. *Geological Society of America Bulletin* 109 (5), 568–579.

- Aloisi, G., Pierre, C., Rouchy, J.M., Foucher, J.P., Woodside, J., 2000. Methane-related authigenic carbonates of eastern Mediterranean sea mud volcanoes and their possible relation to gas hydrate destabilisation. *Earth and Planetary Science Letters* 184 (1), 321–338.
- Babb, I.G., Auster, P.J., Belt, W., Olivier, D., Langton, R.W., Macdonald, I.R., Popenoe, P., Steneck, R.S., 1993. Dual-use of a nuclear powered research submersible – the US-Navy NR-1. *Marine Technology Society Journal* 27 (4), 39–48.
- Bouma, A.H., Roberts, H.H., 1990. Northern Gulf of Mexico continental slope. *Geo-Marine Letters* 10, 177–181.
- Brooks, J.M., Wiesenburg, D.A., Roberts, H., Carney, R.S., MacDonald, I.R., Fisher, C.R., Guinasso, J., N.L., Sager, W.W., McDonald, S.J., Burke, J., Ahron, R.P., Bright, T.J., 1990. Salt, seeps and symbiosis in the Gulf of Mexico. *Eos* 71, 1772–1773.
- Charlou, J.L., Donval, J.P., Zitter, T., Roy, N., Jean-Baptiste, P., Foucher, J.P., Woodside, J., 2003. Evidence of methane venting and geochemistry of brines on mud volcanoes of the eastern Mediterranean Sea. *Deep-Sea Research Part I: Oceanographic Research Papers* 50 (8), 941–958.
- Dimitrov, L., Woodside, J., 2003. Deep sea pockmark environments in the eastern Mediterranean. *Marine Geology* 195 (1–4), 263–276.
- Dimitrov, L.L., 2002. Mud volcanoes – the most important pathway for degassing deeply buried sediments. *Earth-Science Reviews* 59 (1–4), 49–76.
- Feseker, T., Foucher, J.P., Harmegnies, F., 2008. Fluid flow or mud eruptions? Sediment temperature distributions on Hakon Mosby mud volcano, SW Barents Sea slope. *Marine Geology* 247 (3–4), 194–207.
- Fitzsimons, M.F., Dando, P.R., Hughes, J.A., Thiermann, F., Akoumianaki, I., Pratt, S.M., 1997. Submarine hydrothermal brine seeps off Milos, Greece: observations and geochemistry. *Marine Chemistry* 57 (3–4), 325–340.
- Gebrek, A.V., Krylova, E.M., Lein, A.Y., Vinogradov, G.M., Anderson, E., Pimenov, N.V., Cherkashev, G.A., Crane, K., 2003. Methane seep community of the Hakon Mosby mud volcano (the Norwegian Sea): composition and trophic aspects. *Sarsia* 88 (6), 394–403.
- Graue, K., 2000. Mud volcanoes in deepwater Nigeria. *Marine and Petroleum Geology* 17 (8), 959–974.
- Huguen, C., Mascle, J., Woodside, J., Zitter, T., Foucher, J.P., 2005. Mud volcanoes and mud domes of the Central Mediterranean Ridge: near-bottom and in situ observations. *Deep-Sea Research Part I: Oceanographic Research Papers* 52 (10), 1911–1931.
- Joye, S.B., MacDonald, I.R., Montoya, J.P., Peccini, M., 2005. Geophysical and geochemical signatures of Gulf of Mexico seafloor brines. *Biogeosciences* 2 (3), 295–309.
- Judd, A.G., Hovland, M., Dimitrov, L.L., Gil, S.G., Jukes, V., 2002. The geological methane budget at Continental Margins and its influence on climate change. *Geofluids* 2 (2), 109–126.
- Kopf, A.J., 2002. Significance of mud volcanism. *Reviews of Geophysics* 40 (2).
- Kopf, A.J., 2003. Global methane emission through mud volcanoes and its past and present impact on the Earth's climate. *International Journal of Earth Sciences* 92 (5), 806–816.
- Kvenvolden, K.A., Rogers, B.W., 2005. Gaia's breath – global methane exhalations. *Marine and Petroleum Geology* 22 (4), 579–590.
- Kvitek, R.G., Conlan, K.E., Iampietro, P.J., 1998. Black pools of death: hypoxic, brine-filled ice gouge depressions become lethal traps for benthic organisms in a shallow Arctic embayment. *Marine Ecology-Progress Series* 162, 1–10.
- Lance, S., Henry, P., Le Pichon, X., Lallemand, S., Chamley, H., Rostek, F., Faugeres, J.C., Gonthier, E., Olu, K., 1998. Submersible study of mud volcanoes seaward of the Barbados accretionary wedge: sedimentology, structure and rheology. *Marine Geology* 145 (3–4), 255–292.
- Leifer, I., MacDonald, I., 2003. Dynamics of the gas flux from shallow gas hydrate deposits: interaction between oily hydrate bubbles and the oceanic environment. *Earth and Planetary Science Letters* 210 (3–4), 411–424.
- MacAvoy, S.E., Carney, R.S., Fisher, C.R., Macko, S.A., 2002. Use of chemosynthetic biomass by large, mobile, benthic predators in the Gulf of Mexico. *Marine Ecology-Progress Series* 225, 65–78.
- MacDonald, I.R., 1992. Sea-floor brine pools affect behavior, mortality, and preservation of fishes in the Gulf of Mexico: Lagerstätten in the making? *Palaios* 7, 383–387.
- MacDonald, I.R., Buthman, D., Sager, W.W., Peccini, M.B., Guinasso Jr., N.L., 2000. Pulsed oil discharge from a mud volcano. *Geology* 28 (10), 907–910.
- MacDonald, I.R., Reilly, I., J.F., Guinasso Jr., N.L., Brooks, J.M., Carney, R.S., Bryant, W.A., Bright, T.J., 1990. Chemosynthetic mussels at a brine-filled pockmark in the northern Gulf of Mexico. *Science* 248, 1096–1099.
- MacDonald, I.R., Reilly II, J.F., Chu, J., Olivier, D., 1997. NR-1: deep-ocean introduction of new laser line scanner. *Sea Technology* 38 (2), 59–64.
- Milkov, A., Vogt, P., Cherkashev, G., Ginsburg, G., Chernova, N., Andriashev, A., 1999. Sea-floor terrains of Hakon Mosby Mud Volcano as surveyed by deep-tow video and still photography. *Geo-Marine Letters* 19 (1–2), 38–47.
- Milkov, A.V., 2000. Worldwide distribution of submarine mud volcanoes and associated gas hydrates. *Marine Geology* 167 (1–2), 29–42.
- Neurauter, T.W., Roberts, H.H., 1994. 3 Generations of Mud Volcanoes on the Louisiana Continental-Slope. *Geo-Marine Letters* 14 (2–3), 120–125.
- Nix, E., Fisher, C., Vodenichar, J., Scott, K., 1995. Physiological ecology of a mussel with methanotrophic endosymbionts at three hydrocarbon seep sites in the Gulf of Mexico. *Marine Biology* 122, 605–617.
- Olu-Le Roy, K., Sibuet, M., Fiala-Medionni, A., Gofas, S., Salas, C., Mariotti, A., Foucher, J.P., Woodside, J., 2004. Cold seep communities in the deep eastern Mediterranean Sea: composition, symbiosis and spatial distribution on mud volcanoes. *Deep-Sea Research Part I: Oceanographic Research Papers* 51 (12), 1915–1936.
- Parsons-Hubbard, K.M., Powell, E.N., Raymond, A., Walker, S.E., Brett, C., Ashton-Alcox, K., Shepard, R.N., Krause, R., Deline, B., 2008. The taphonomic signature of a brine seep and the potential for Burgess Shale style preservation. *Journal of Shellfish Research* 27 (1), 227–239.
- Parsons, B.S., Vogt, P.R., Hafliadon, H., Jung, W.Y., 2005. Sidescan and video exploration of the Storegga slide headwall region by submarine NR-1. *Marine Geology* 219 (2–3), 195–205.
- Peckmann, J., Thiel, V., 2004. Carbon cycling at ancient methane-seeps. *Chemical Geology* 205 (3–4), 443–467.
- Prior, D.B., Doyle, E.H., Kaluza, M.J., 1989. Evidence for sediment eruption on deep sea floor, Gulf of Mexico. *Science* 243, 517–519.
- Reilly, J.F., MacDonald, I.R., Biegert, E.K., Brooks, J.M., 1996. Geologic controls on the distribution of chemosynthetic communities in the Gulf of Mexico. In: Schumacher, D., Abrams, M.A. (Eds.), *Hydrocarbon Migration and its Near-surface Expression*. Amer. Assoc. Petrol. Geol. Amer. Assoc. Petrol. Geol., Tulsa, OK, pp. 38–61.
- Roberts, H.H., Carney, R.S., 1997. Evidence of episodic fluid, gas, and sediment venting on the northern Gulf of Mexico continental slope. *Economic Geology and the Bulletin of the Society of Economic Geologists* 92 (7–8), 863–879.
- Roberts, H.H., Neurauter, T.W., 1990. Direct observations of a large active mud vent on the Louisiana continental slope. *American Association of Petroleum Geologists Bulletin* 74, 1508.
- Sager, W.W., MacDonald, I.R., Hou, R.S., 2003. Geophysical signatures of mud mounds at hydrocarbon seeps on the Louisiana continental slope, northern Gulf of Mexico. *Marine Geology* 198 (1–2), 97–132.
- Sass, A.M., Sass, H., Coolen, M.J.L., Cypionka, H., Overmann, J., 2001. Microbial communities in the chemocline of a hypersaline deep-sea basin (Urania basin, Mediterranean Sea). *Applied and Environmental Microbiology* 67 (12), 5392–5402.
- Shilov, V.V., Druzhinina, N.I., Vasilenko, L.V., Krupskaya, V.V., 1999. Stratigraphy of sediments from the Hakon Mosby Mud Volcano Area. *Geo-Marine Letters* 19 (1–2), 48–56.
- Shokes, R.F., Trabant, P.K., Preseley, B.J., Reid, D.F., 1977. Anoxic, hypersaline basin in the northern Gulf of Mexico. *Science* 196, 1443–1446.
- Smith, E.B., Scott, K.M., Nix, E.R., Korte, C., Fisher, C.R., 2000. Growth and condition of seep mussels (*Bathymodiolus childressi*) at a Gulf of Mexico Brine Pool. *Ecology* 81 (9), 2392–2403.
- Taylor, J.D., Glover, E.A., 2006. Lucinidae (Bivalvia) – the most diverse group of chemosymbiotic molluscs. *Zoological Journal of the Linnean Society* 148 (3), 421–438.
- Woodside, J.M., Volgin, A.V., 1996. Brine pools associated with Mediterranean Ridge mud diapirs: an interpretation of echo-free patches in deep tow sidescan sonar data. *Marine Geology* 132 (1–4), 55–61.
- Yakimov, M.M., Giuliano, L., Crisafi, E., Chernikova, T.N., Timmis, K.N., Golyshin, P.N., 2002. Microbial community of a saline mud volcano at San Biagio-Belpasso, Mt. Etna (Italy). *Environmental Microbiology* 4 (5), 249–256.